Review

The real-time polymerase chain reaction

Mikael Kubista [a,*], José Manuel Andrade [b],
Martin Bengtsson [a,c], Amin Forootan [d], Jiri Jonák [e],
Kristina Lind [a,f], Radek Sindelka [e], Robert Sjöback [a],
Björn Sjögreen [d], Linda Strömbom [a], Anders Ståhlberg [a,g],
Neven Zoric [a]

[a] TATAA Biocenter, Medicinargatan 7B, 405 30 Göteborg, Sweden
[b] Department of Analytical Chemistry, University of A Coruna, A Zapateira s/n, E-15071 A Coruna, Spain
[c] Department of Experimental Medical Science, Lund University, 221 84 Lund, Sweden
[d] MultiD Analyses AB, Lotsgatan 5A, 414 58 Gothenburg, Sweden
[e] Laboratory of Gene Expression, Institute of Molecular Genetics, Academy of Sciences of the Czech Republic, Flemingovo n. 2, 16637 Prague 6, Czech Republic
[f] Department of Chemistry and Biosciences, Chalmers University of Technology, Sweden
[g] Stem Cell Center, Lund University, BMC, B10, Klinikgatan 26, 22184 Lund, Sweden

Abstract

The scientific, medical, and diagnostic communities have been presented the most powerful tool for quantitative nucleic acids analysis: real-time PCR [Bustin, S.A., 2004. A–Z of Quantitative PCR. IUL Press, San Diego, CA]. This new technique is a refinement of the original Polymerase Chain Reaction (PCR) developed by Kary Mullis and coworkers in the mid 80:ies [Saiki, R.K., et al., 1985. Enzymatic amplification of β-globin genomic sequences and restriction site analysis for diagnosis of sickle cell anemia, Science 230, 1350], for which Kary Mullis was awarded the 1993 year's Nobel prize in Chemistry. By

* Corresponding author. Tel.: +46 31 7733926; fax: +46 31 7733910.
  E-mail address: mikael.kubista@tataa.com (M. Kubista).

PCR essentially any nucleic acid sequence present in a complex sample can be amplified in a cyclic process to generate a large number of identical copies that can readily be analyzed. This made it possible, for example, to manipulate DNA for cloning purposes, genetic engineering, and sequencing. But as an analytical technique the original PCR method had some serious limitations. By first amplifying the DNA sequence and then analyzing the product, quantification was exceedingly difficult since the PCR gave rise to essentially the same amount of product independently of the initial amount of DNA template molecules that were present. This limitation was resolved in 1992 by the development of real-time PCR by Higuchi et al. [Higuchi, R., Dollinger, G., Walsh, P.S., Griffith, R., 1992. Simultaneous amplification and detection of specific DNA-sequences. Bio-Technology 10(4), 413–417]. In real-time PCR the amount of product formed is monitored during the course of the reaction by monitoring the fluorescence of dyes or probes introduced into the reaction that is proportional to the amount of product formed, and the number of amplification cycles required to obtain a particular amount of DNA molecules is registered. Assuming a certain amplification efficiency, which typically is close to a doubling of the number of molecules per amplification cycle, it is possible to calculate the number of DNA molecules of the amplified sequence that were initially present in the sample. With the highly efficient detection chemistries, sensitive instrumentation, and optimized assays that are available today the number of DNA molecules of a particular sequence in a complex sample can be determined with unprecedented accuracy and sensitivity sufficient to detect a single molecule. Typical uses of real-time PCR include pathogen detection, gene expression analysis, single nucleotide polymorphism (SNP) analysis, analysis of chromosome aberrations, and most recently also protein detection by real-time immuno PCR.

© 2006 Published by Elsevier Ltd.

Contents

1. Real-time PCR basics

1.1. PCR amplification

PCR is performed on a DNA template, which can be single or double-stranded. Also needed are two oligonucleotide primers that flank the DNA sequence to be amplified, dNTPs, which are the four nucleotide triphosphates, a heat-stable polymerase, and magnesium ions in the buffer. The reaction is performed by temperature cycling. High temperature is applied to separate (melt) the strands of the double helical DNA, then temperature is lowered to let primers anneal to the template, and finally the temperature is set around 72 °C, which is optimum for the polymerase that extends the primers by incorporating the dNTPs (Fig. 1).

The melting shall be sufficient to fully separate the strands of the template, because partially strand separated structures will rapidly reanneal when temperature is dropped and will not be primed. The required melting temperature and duration of melting depends on the length and sometimes the sequence of the template and also on the instrument and the reaction containers used. With short amplified sequences, also called amplicons, and containers with rapid heat transfer, such as glass capillaries, it may be sufficient to touch 95 °C and then immediately start cooling. It may be necessary to heat more thoroughly during the first few cycles, because the original template is typically much longer than the amplicons that dominate later. Also, some hot-start polymerases require extensive heat activation.

The annealing temperature depends on the primers. Theoretically it shall be a few degrees below the melting temperature of the two primers (which shall be designed to have the same or similar melting temperatures), in order for them to form stable complexes with the targeted sequences but not with any other sequences. Several free and commercial softwares are available to estimate primer melting temperatures (http://frodo.wi.mit.edu/..cgi-bin/primer3/primer3_www.cgi, http://www.premierbiosoft.com/netprimer). These, however, do not account for the stabilizing effect of the
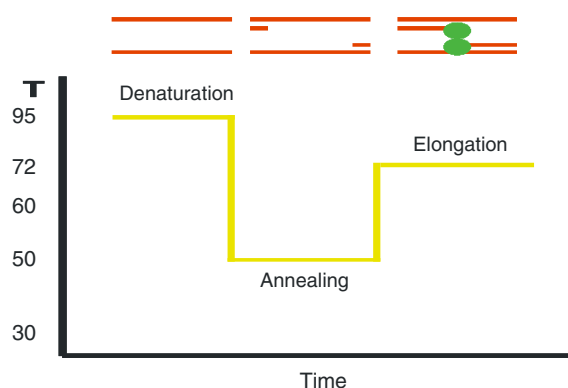

Fig. 1. The PCR temperature cycle: (1) the temperature is raised to about 95 °C to melt the double stranded DNA, (2) the temperature is lowered to let primers anneal, (3) the temperature is set to 72 °C to let the polymerase extend the primers.

polymerase, which binds the annealed primer and stabilizes the complex. In fact, the mechanism is probably that the polymerase binds the primer first and then the polymerase-primer complex binds target DNA.

Optimum temperature for Taq polymerase is about 72 °C, which is the elongation temperature used in most three-step PCR protocols. But it does not seem very important, and some protocols, particularly those based on Taqman probes (see below) elongate at 60 °C (Holland et al., 1991). Using elevated elongation temperature is probably more important to melt any secondary structures that may form in the template and may block extension. In real-time PCR amplicons are typically short with limited capability to fold. But sequential runs of guanines, even only 2–3 consecutive guanines, may fold the template into a tetraplex structure, which is exceedingly stable and cannot be transcribed by the polymerase (Simonson et al., 1998). Guanine tetraplexes form exclusively in the presence of K^+ ions (Simonsson, 2001), and the problem can be avoided by using K^+ free PCR buffer. Self complementary regions in the template can also cause problems by folding into hair-pins and other structures that may interfere with the extension. The same sequence features cause problems also if present in the primers. Complementarity between the primers, particularly in their 3′-ends, causes complications by forming aberrant PCR products called primer–dimers. Avoiding the formation of primer–dimer products is very important for quantitative PCR analysis of samples that contain only few target molecules because the PCR of the target and the PCR forming primer–dimers compete.

1.2. Real-time monitoring of PCR

Real-time PCR also needs a fluorescent reporter that binds to the product formed and reports its presence by fluorescence (Fig. 2). A number of probes and dyes are available and they are described in the next chapter. For now it is sufficient to know that the reporter generates a fluorescence signal that reflects the amount of product formed. During the initial cycles the signal is weak and cannot be distinguished from the background (Fig. 3). As the amount of product accumulates a signal develops that initially increases exponentially. Thereafter the signal levels off and saturates. The signal saturation is due to the reaction running out of some critical component. This can be the primers, the reporter, or the dNTPs (Kubista et al., 2001). Also the number of polymerase molecules may be limiting, in which case the exponential amplification goes over to linear amplification. It is worth noting that in a typical real-time PCR experiment all response curves saturate at the same level. Hence, end-point PCR measurements tell us nothing about the initial amounts of target molecules that were present in the samples; they only distinguish a positive from a negative sample. On the other hand the response curves are separated in the growth phase of the reaction. This reflects the difference in their initial amounts of template molecules. The difference is quantified by comparing the number of amplification cycles required for the samples' response curves to reach a particular threshold fluorescence signal level. The number of cycles required to reach threshold is called the CT value. The amplification response curves are expected to be parallel in the growth

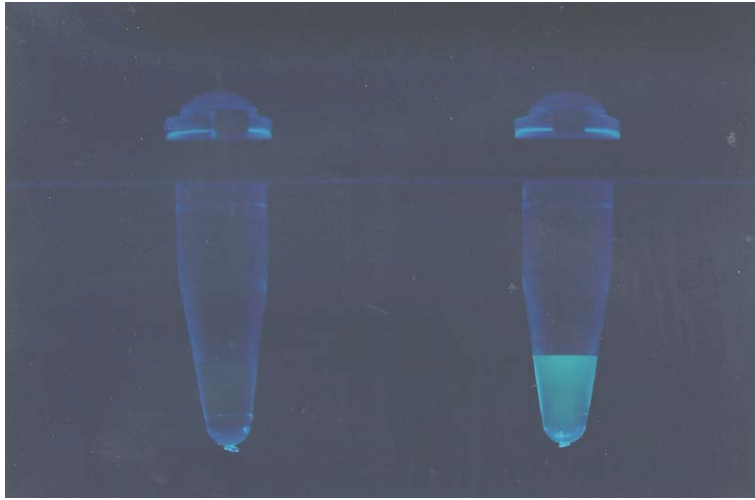Fig. 2. Fluorescence from hybridized probe. Both PCR tubes contain DNA and probe. In the left tube the probe and the DNA are not complementary and the probe does not bind, while in the right tube the probe and the DNA are complementary.
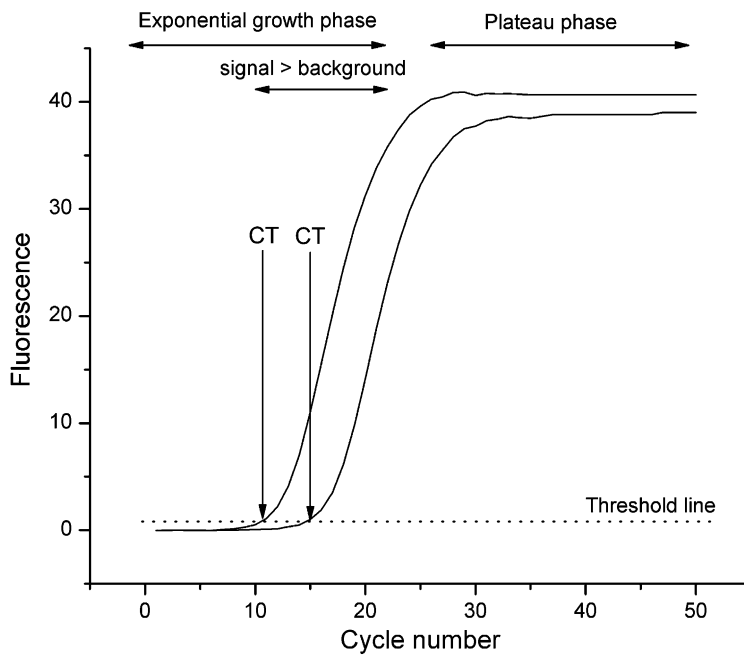

Fig. 3. Real-time PCR response curves. A threshold level is set sufficiently above background and the number of cycles required to reach threshold, CT, are registered.

phase of the reaction, and the setting of the threshold level should therefore not be critical. Different instrument softwares use different methods and algorithms to select the threshold, and most also let the user set it manually. The setting is therefore somewhat arbitrary and it does not affect significantly the differences between CT values, though it affects the values of the individual CTs. These are also affected by the setting of the instrument (filter, channel, gain, etc.). Hence, one should avoid comparing individual CT values between experiments, and include one reference per run to which all the other response curves can be related.

Assuming that the PCR is 100% efficient the ratio between the initial numbers of template copies in two samples is given by

$$\frac{[N_0]_A}{[N_0]_B} = 2^{(CT_B - CT_A)} \tag{1}$$

$[N_0]_A$ and $[N_0]_B$ are the initial numbers of template molecules in samples A and B, and CT_A and CT_B are the corresponding CT values. Suppose the response of sample A appears four cycles later than the response of sample B, i.e., four additional PCR cycles were needed to reach the same threshold level, sample A should initially have contained $2 \times 2 \times 2 \times 2 = 16$ times less template molecules than sample B. Note that the signal for the sample that initially contained less molecules requires higher number of amplification cycles and, hence, develops later.

If the PCR is not perfect, which it almost never is, the efficiency of the PCR enters the equation as

$$\frac{[N_0]_A}{[N_0]_B} = (1 + E)^{(CT_B - CT_A)} \tag{2}$$

Let say that the PCR is 90% efficient, which is quite typical when using biological samples. Four cycles difference between the two amplification curves then reflects a ratio of $(1 + 0.9)^4 = 13$ between the initial numbers of template copies in samples B and A. 16 and 13 are quite different estimates, emphasizing the importance of estimating the PCR efficiency and taking it into account.

The efficiency of a PCR assay can be estimated from a standard curve based on serial dilution of a standard, which can be a purified PCR product or a purified plasmid that contains the target sequence (Fig. 4) (Rutledge and Cote, 2003). The CT values of the diluted standards are read out, and plotted versus the logarithm of the samples' concentrations, number of template copies or dilution factor. The data are fitted to the equation:

$$CT = k \times \log(N_0) + CT(1) \tag{3}$$

The PCR efficiency is calculated from the slope as:

$$E = 10^{-\frac{1}{k}} - 1 \tag{4}$$

The intercept of the standard curve corresponds to the CT(1) of a diluted standard containing only a single target molecule.
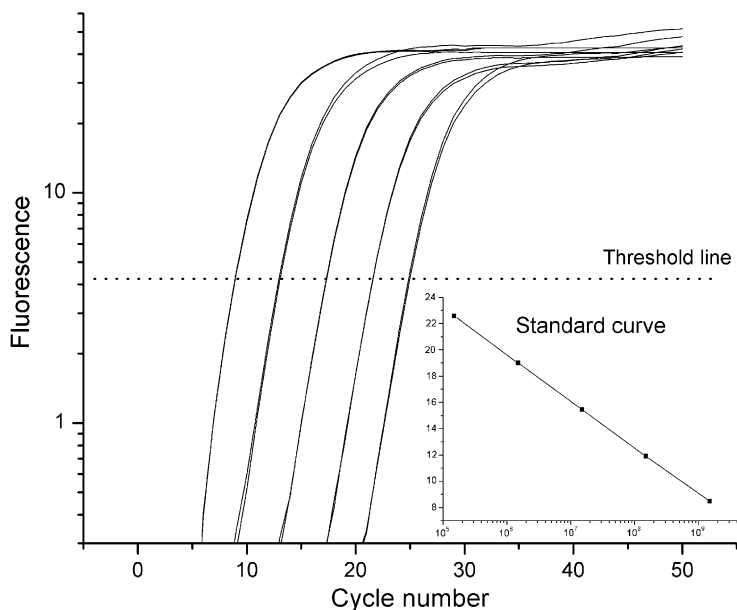
Fig. 4. Real-time PCR standard curve. Real-time PCR response curves shown in logarithmic scale for five standard samples. The crossing points with threshold line are the CT values. In the inset the CT values are plotted vs. the logarithm of the initial number of template copies in the standard samples.

The standard dilution series (briefly, standard curve) approach gives a good estimate of the efficiency of the PCR assay. But, most importantly, it does not tell us anything about the effect of the matrix of the real test sample. Biological samples are complex and may contain inhibitory substances that are not present in standards based on purified template, and this may reduce the PCR efficiency. Examples of common PCR inhibitors are heme, heparin, IgG, and lipids (Akane et al., 1994; Izraeli et al., 1991; Al-Soud et al., 2000). If there is enough sample it may be purified extensively and then diluted, which reduces inhibition. But some inhibitors are hard to remove by dilution. In such cases one may estimate the PCR efficiency of the test sample by either serial dilution of the sample or by the method of standard additions (Ståhlberg et al., 2003).

Some authors suggest estimating PCR efficiencies from the real-time PCR response curves. The idea is indeed attractive because it would allow more precise determination, and in an extension also absolute determination, of the number of target molecules in a sample (Rutledge, 2004; Van et al., 2005). Particularly when using dyes the rise of the amplification response curve is exceedingly difficult to model, because the amount of dye bound per amplicon changes when the DNA concentration increases, and the fluorescence of the bound dye depends on the binding ratio. But recently some important advances have been made and reliable corrections for PCR efficiency from the amplification curves may become reality sometime in the future (Rutledge, 2005).

1.3. Fluorescence reporters

Today fluorescence is exclusively used as the detection method in real-time PCR. Both sequence specific probes and non-specific labels are available as reporters. In his initial work Higuchi used the common nucleic acid stain ethidium bromide, which becomes fluorescent upon intercalating into DNA (Higuchi et al., 1992). Classical intercalators, however, interfere with the polymerase reaction, and asymmetric cyanine dyes such as SYBR Green I and BEBO have become more popular (Fig. 5) (Zipper et al., 2004; Bengtsson et al., 2003). Asymmetric cyanines have two aromatic systems containing nitrogen, one of which is positively charged, connected by a methine bridge. These dyes have virtually no fluorescence when they are free in solution due to vibrations engaging both aromatic systems, which convert electronic excitation energy into heat that dissipates to the surrounding solvent. On the other hand the dyes become brightly fluorescent when they bind to DNA, presumably to the minor groove, and rotation around the methine bond is restricted (Nygren et al., 1998). In PCR the fluorescence of these dyes increases with the amount of double stranded product formed, though not strictly in proportion because the dye fluorescence depends on the dye:base binding ratio, which decreases during the course of the reaction. The dye fluorescence depends also to some degree on the DNA sequence. But a certain amount of a particular double-stranded DNA target, in the absence of significant amounts of other double-stranded DNAs, gives rise to the same fluorescence every time. Hence, the dyes are excellent for quantitative real-time PCR when samples are compared at the same level of fluorescence in absence of interfering DNA. Although minor groove binding dyes show preference for runs of AT base-pairs (Jansen et al., 1993), asymmetric cyanines are considered sequence non-specific reporters in real-time PCR. They give rise to fluorescence signal in the presence of any double stranded DNA including undesired primer–dimer products. Primer–dimer formation interferes with the formation of specific products because of competition of the two reactions for reagents and may lead to erroneous readouts. It is therefore good practice to control for primer–dimer formation. This can be done by melting curve analysis after completing the PCR. The temperature is then gradually increased and the fluorescence is measured as function of temper-
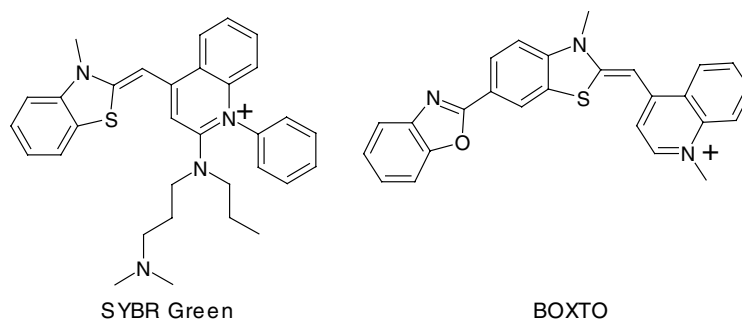

Fig. 5. The asymmetric cyanine dyes SYBR Green and BOXTO.

ature. The fluorescence decreases gradually with increasing temperature because of increased thermal motion which allows for more internal rotation in the bound dye (Nygren et al., 1998). However, when the temperature is reached at which the double stranded DNA strand separates the dye comes off and the fluorescence drops abruptly (Fig. 6) (Ririe et al., 1997). This temperature, referred to as the melting temperature, T_m, is easiest determined as the maximum of the negative first derivative of the melting curve. Since primer–dimer products typically are shorter than the targeted product, they melt at a lower temperature and their presence is easily recognized by melting curve analysis.

Labeled primers and probes are based on nucleic acids or some of their synthetic analogues such as the peptide nucleic acids (PNA) (Egholm et al., 1992) and the locked nucleic acids (LNA) (Costa et al., 2004). The dye labels are of two kinds: (i) fluorophores with intrinsically strong fluorescence, such as fluorescein and rhodamine derivatives (Sjöback et al., 1995), which through structural design are brought into contact with a quencher molecule, and (ii) fluorophores that change their fluorescence properties upon binding nucleic acids (Fig. 7). Examples of probes with two dyes are the hydrolysis probes, popularly called Taqman probes (Holland et al., 1991), which can be based either on regular oligonucleotides or on LNA (Braasch and Corey, 2001), Molecular Beacons (Tyagi and Kramer, 1996; Tyagi et al., 1998), Hybridization probes (Caplin et al., 1999), and the Lion probes (http://www.biotools.net). The dyes form a donor–acceptor pair, where the donor dye is excited and transfers its energy to the acceptor molecule if it is in proximity. Originally the acceptor molecule was also a dye, but today quencher molecules are more
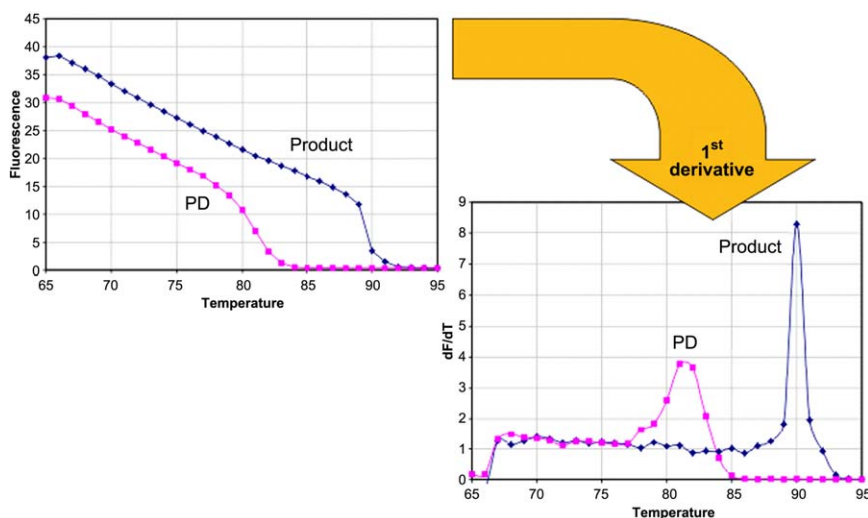

Fig. 6. Melting curve analysis. Dye fluorescence drops rapidly when the DNA melts. The melting point is defined as the inflection point of the melting curve, which is easiest determined as the maximum in the negative 1st derivative of the melting curve. The amplicon produced from the targeted product is typically longer and melts at higher temperature than the primer–dimers.
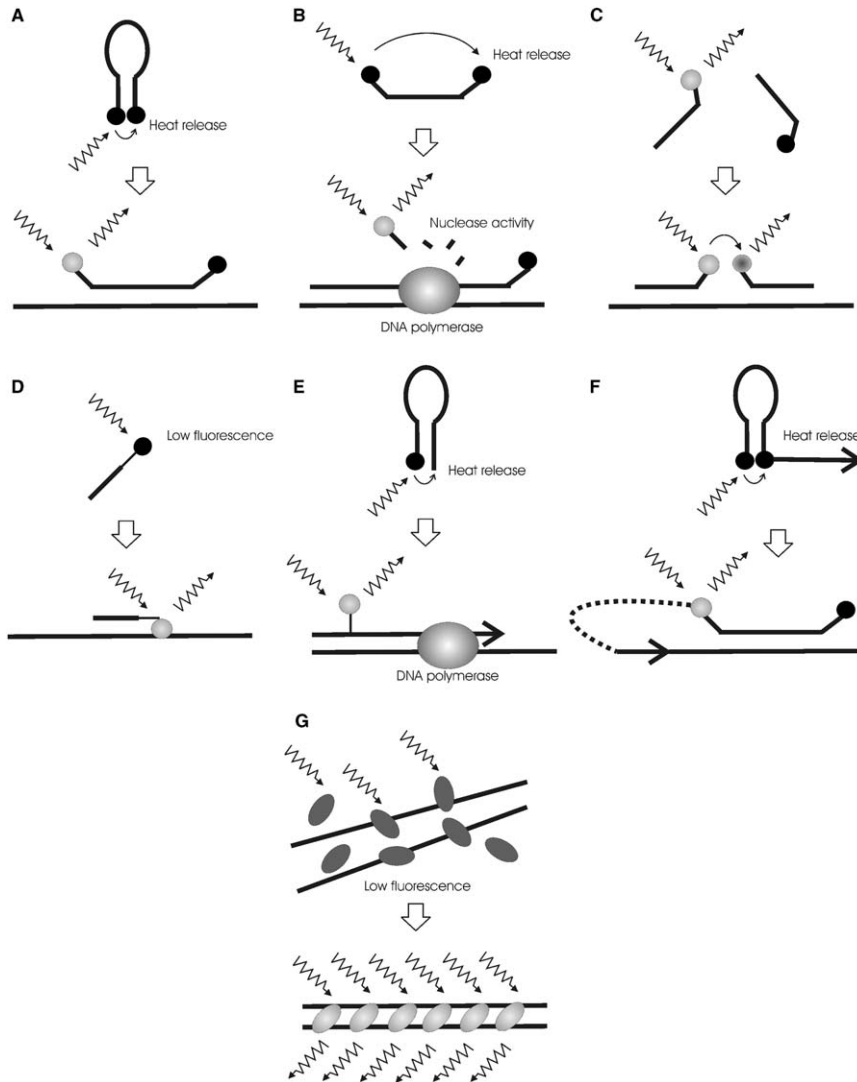
Fig. 7. Mechanisms of reporters used in real-time PCR: (A) the molecular beacon, (B) the Taqman probe, (C) the hybridization probes, (D) the LightUp probe, (E) the simple probe, (F) scorpion primer, (G) sequence non-specific dyes (SYBR Green/BOXTO).

popular (Wilson and Johansson, 2003). Energy transfer and quenching are distance dependent and structural rearrangement of the probe, or, in the case of hydrolysis probes, degradation, change the distance between the donor and acceptor and, hence, the fluorescence of the system.

Probes based on a single dye, whose fluorescence changes upon binding target DNA include the LightUp probes (Svanvik et al., 2000), AllGlo probes (http://

www.allelogic.com), Displacement probes (Li et al., 2002), and the Simple probes (http://www.idahotech.com/itbiochem/simpleprobes.html). Chemical modifications and alterations of the oligonucleotide backbone are employed in some probes to improve the binding properties to the target template. This makes it possible to use shorter probes, which is advantageous for the detection of targets with short conserved regions such as retroviruses. LightUp probes have a neutral peptide nucleic acid (PNA) backbone that binds to DNA with greater affinity than normal oligonucleotides. The LightUp probes are 10–12 bases, which is short compared to normal oligonucleotide probes that are usually at least 25 bases (http://www.lightup.se). LNA-probes make use of modified nucleotides to enhance binding affinity. MGB-probes are hydrolysis probes with a minor groove binding molecule attached to the end of the probe to increase affinity for DNA, which makes it possible to use shorter probes (Kutyavin et al., 2000). Examples of modified primers include: Scorpion primers (Whitcombe et al., 1999), LUX primers (Nazarenko et al., 2002), Ampliflour primers (Uehara et al., 1999), and the QZyme system (BD QZyme™ Assays for Quantitative PCR, 2003).

As long as a single target is detected per sample there is not much of a difference in using a dye or a probe. Assay specificity is in both cases determined by the primers. Probes do not detect primer–dimer products, but using non-optimized probe assays is hiding the problem under the rug. If primer–dimers form they cause problems whether they are seen or not. In probe based assays, particularly when high CT values are obtained, one should verify the absence of competing primer–dimer products. The traditional way is by gel electrophoresis. Recently, an alternative approach was proposed based on the BOXTO dye. BOXTO is a sequence non-specific double-stranded DNA binding dye that has distinct spectral characteristics to fluorescein and can be used in combination with FAM based probes. The BOXTO and the probe signals are detected in different channels of the real-time PCR instrument. While the probe reflects formation of the targeted product as usual, the BOXTO dye also reports the presence of any competing primer–dimer products, which can be identified by melting curve analysis (Lind et al., in press).

The great advantage of probes is for multiplexing, where several products are amplified in the same tube and detected in parallel (Wittwer et al., 2001). Today multiplexing is mainly used to relate expression of reporter genes to that of an exogenous control gene in diagnostic applications (Mackya, 2004), and for single nucleotide polymorphism (SNP) and mutation detection studies (Mhlanga and Malmberg, 2001; Mattarucchi et al., 2005). Multiplex assays are more difficult to design because when products accumulate the parallel PCR reactions compete for reagents. To minimize competition limiting amounts of primers must be used. Also, primer design is harder, because complementarity must be avoided between all the primers. Multiplex assays can be based either on probes or on labeled primers, where labeled primers usually give rise to signal from primer–dimer products, while probes do not.

The different probing technologies have their advantages and limitations. Dyes are cheaper than probes but they do not distinguish between products. Hairpin forming probes have the highest specificity, because the formation of the hairpin competes with the binding to mismatched targets. This makes them most suitable for

SNP and multi-site variation (MSV) analysis (Bonnet et al., 1999). Hydrolysis probes require two-step PCR to function properly, which is not optimal for the polymerase reaction, and short amplicons are necessary to obtain reasonable amplification efficiencies. But they are easier to design than hairpin forming probes and an 80% success rate was recently reported (Kubista, 2004).

In summary, a 'good' probe, independent of chemistry, should have low background fluorescence, high fluorescence upon target formation (high signal to noise ratio), and high target specificity. The dyes' excitation and emission spectra are important parameters to consider when designing multiplex reactions. Spectral overlap in excitation and emission should be minimized to keep cross-talk to a minimum.

1.4. Real-time PCR instruments

Today many instrument platforms are available for quantitative real-time PCR. The main differences between them are the excitation and emission wavelengths that are available, speed, and the number of reactions that can be run in parallel (Kubista and Zoric, 2004). Reaction containers also differ. Most popular are 96-well microtiter plates, which are becoming standardized and therefore available from multiple vendors. These are used in the Applied Biosystems 7300 and 7500 instruments (http://www.appliedbiosystems.com), the Exicycler from Bioneer (http://www.bioneer.co.kr), the Chromo4, the DNAEngine Opticon, the iCycler, the iQ, the MyiQ, and the iQ5 from BioRad (http://discover.bio-rad.com), the RealPlex from Eppendorf (http://www.eppendorf.com/mastercycler/index.html), the Mx3000p, the Mx3005p, and the Mx4000 from Stratagene (http://www.stratagene.com), and the Quantica from Techne (http://www.techne.com/CatMol/quantica.htm). Currently there are two 384-well plates instruments available on the market: the ABI PRISM 7900HT from Applied Biosystems (http://www.appliedbiosystems.com), and the LightCycler 480 system from Roche (http://www.roche-applied-science.com). For very high throughput we see an interesting development at Biotrove who have a through-hole array platform, called OpenArray™, enabling massively parallel real-time PCR. Passive microfluidics based on surface tension differentials load and retain in isolation 3072 33 nl reaction volumes in a footprint the size of microscope slide. Samples and primer pairs can be loaded into the OpenArray to give the user maximum flexibility in the number of transcripts measured per sample. Three such OpenArray plates can be run simultaneously in BioTrove's real-time PCR instrument enabling the study of up to 64 transcripts in 144 samples, or any combination thereof, equal to 9216 real-time PCR reactions (Brenan and Morrison, 2005) (http://www.biotrove.com).

The Rotor-Gene 3000 (4-Channel) and 6000 (6-Channel) from Corbett Research are based on a rotor platform to achieve the highest temperature uniformity between samples. They use plastic tubes, which are rather inexpensive (http://www.corbettresearch.com). The LightCycler from Roche uses glass capillaries (http://www.roche-applied-science.com). These have excellent optical properties, but are somewhat more expensive. But recently cheaper replica made of plastics has appeared. The Cepheid SmartCycler uses special containers for cycling (http://www.cepheid.com).

The instrument is designed for field testing, and can run several different assays that must not even be started simultaneously in parallel. The InSyte from Biobank has 96 independent wells, seven color multiplexing and very fast cycling by using special conductive plastic containers (http://www.biobank.co.kr/pcr/insyte.shtml). The fastest real-time PCR instrument of them all is the SuperConvector from AlphaHelix that runs at elevated G-forces, which cause turbulent flow and thereby rapid mixing resulting in extremely fast heat-transfer (http://www.alphahelix.com/pages/super-convector.html). For these more sophisticated instruments the higher cost for containers is probably negligible anyway. Then there is the very small DT-322 instrument from DNA Technology (http://www.dna-technology.com/catalog/ob_dt322_en.shtml), and a fiber optics based Line-Gene II from Bioer (http://www.bioer.com.cn/en/shengming_66pcr.htm). Fluidigm develops nanofluidic chips called dynamic arrays for QPCR. The instrument's footprint is W30'' × D30'' × H39''. It has five excitation filters, five emission filters, and a CCD that images the entire chip. Current chips are 48/48 dynamic arrays that yield 2304 real-time PCR reactions each being 10 nl (http://www.fluidigm.com) (A nanofluidic chip for absolute quantification of target nucleic acid sequences, Pharmaceutical Discovery October 1, 2005). Even a notebook real-time PCR instrument has been described (Belgrader et al., 2001). As for performance, sensitivity and accuracy the conventional instruments are virtually equivalent. Also the instrument softwares are pretty much the same at least concerning the basic features, such as setting up the experiment and specifying protocols, and simple pre-processing and processing of data, including base-line subtraction and calculating threshold cycle numbers. The prices for the instruments vary quite substantially, mainly depending on throughput and the number of colors they can handle. Unless you plan to do multiplexing and are not running a core facility, you can save a lot of money and still do excellent real-time PCR on anyone of the less expensive instruments.

2. Gene expression measurements

Before a gene expression measurement can be performed by real-time PCR, the mRNA in the sample must be copied to cDNA by reverse transcription (RT) (Fig. 8). The RT step is critical for sensitive and accurate quantification, since the amounts of cDNAs produced must correctly reflect the input amounts of the mRNAs. Comparing the technical reproducibilities of the RT reaction and the PCR it was found that the RT reaction contributes with most of the variation to the experimental determination of mRNA quantities (Ståhlberg et al., 2004a). Hence, it was concluded that substantially higher experimental accuracy is obtained when performing replicates starting with the RT reaction than when splitting the samples after the RT step to perform real-time PCR replicates only.

In an RT reaction RNA molecules are transcribed to DNA copies by a reverse transcriptase. The reaction can proceed without added primer, but higher efficiency is obtained when primers are added (Ståhlberg et al., 2004a). The three basic priming strategies are based on oligo(dT) primer, random sequence primers, and gene
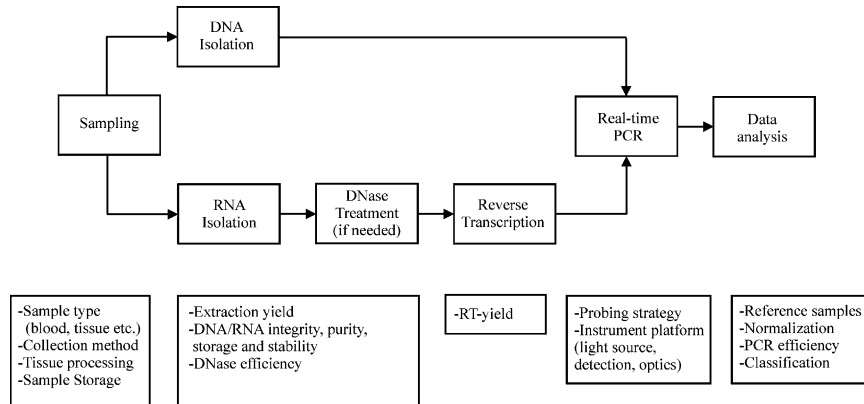
Fig. 8. Scheme of RNA and DNA analysis from biological samples. Sources of variation are indicated.
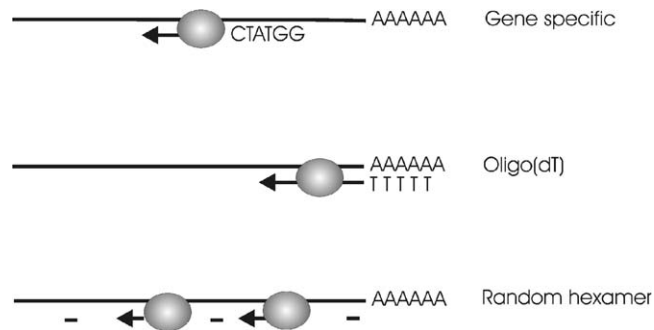

Fig. 9. RT priming strategies.

specific primers (Fig. 9). Oligo(dT) primers hybridize to the poly(A) tail present in most eukaryotic mRNAs and will initiate reverse transcription from the very beginning (3′-end) of the mRNA. This is important advantage if the cDNA shall be cloned. But for expression analysis this may be a disadvantage, because the transcription may not reach the PCR target sequence if the mRNA is not intact because of degradation, and a bias for amplicons located close to the mRNA 3′-end may be introduced. Particularly if the mRNA samples studied are of varying quality this may be a problem. Another limitation is that mRNAs without A-tails, such as histone genes in most eukaryotes, and most prokaryotic genes, are not transcribed. Ribosomal RNA and transfer RNA are not copied either, which precludes using rRNAs as internal standard. A variant are anchored oligo(dT) primers, which are oligothymines with one or two non-thymine bases in the 3′-end. These were initially designed for cloning purposes, but may be useful in diagnostic cDNA synthesis by anchoring the primer to the start of the A-tail. This results in homogeneous transcripts of each mRNA, which some vendors claim improves reproducibility.

One advantage of oligo(dT) primers is that their target sequence is a run of adenines, which does not fold into higher order structures. Oligo(dT) priming is therefore expected to be more efficient and less dependent on temperature than other priming strategies. Random sequence primers are short oligomers of all possible sequences. They are usually six (random hexamers) or nine (random nonamers) bases long. They are produced by random sequence synthesis, by essentially adding a blend of all four nucleotides in each step of the oligonucleotide synthesis. This gives rise to essentially all sequences, although some bias is expected due to variations in coupling efficiencies, where particularly some longer nucleotide runs are synthesized in poor yields. However, this bias is not likely to be important for their use as RT primers. Random sequence primers will copy all RNA, including tRNA, rRNA, and mRNA. It is the priming strategy of choice if rRNA shall be used as reference and for total reverse transcription of prokaryotic mRNA. Random nonamers bind stronger to target than random hexamers and may be preferred in high temperature RT protocols. On the other hand, they require access to larger regions in the target, which requires the mRNA to be more unfolded. Random oligomer priming may give rise to multiple transcripts, and may at least in theory give RT yields exceeding 100%. Transcription is expected to be initiated at more sites on longer RNAs than on shorter ones, and transcription yields will also depend on the RNAs secondary and tertiary structures. For total reverse transcription of RNA of lower quality, such as fixed and archival samples, random oligomers are preferred to oligo(dT) primers, because they are more likely to yield transcripts that extend past the PCR target sequences. For total reverse transcription, when it is important to copy as many of the different mRNAs as possible, one may use a blend of random oligomers and oligo(dT) primers. Third option is to use sequence specific primers. This is the preferred strategy when a limited number of mRNAs shall be analyzed. The hybridization of specific primers to mRNA is highly sequence dependent because of the folding of mRNA to secondary and tertiary structures. In non-purified samples access may also be limited by bound proteins. The primer must target an accessible sequence. What regions in the mRNA are accessible for priming cannot be predicted by inspection of the mRNA sequence only. It depends also on temperature. At elevated temperatures more sequence regions are accessible, which is the reason heat-stabile reverse transcriptases are gaining popularity. Software, such as *m*-fold, can aid in primer design by predicting the folded structures of RNAs (http://molbio.info.nih.gov/molbionih/mfold.html). However, structure prediction is only feasible for a few hundred base-pairs, while native mRNAs are several thousands or tens of thousands of base-pairs. A practical approach is to test a set of primers, and then go with the one that gave highest yields. Designing only one primer and hoping for the best, the yield may not be higher than when using random sequence oligomers or poly(dT) primers (Ståhlberg et al., 2004a). The RT primer may also be used as the reverse primer in the PCR, reducing the total number of primers needed. The RT and real-time PCR reactions can then be combined into a one-step RT-PCR reaction. This is convenient when analyzing only one or a few genes, and it reduces the risk of cross-contamination. However, optimal reaction conditions for the RT and real-time PCR are usually

somewhat different, and one-step reactions tend to be less sensitive than the regular two-step approach (Ståhlberg et al., 2004a; Bustin, 2002).

Several reverse transcriptases are today available commercially. Most are engineered forms of either the Moloney Murine Leukemia Virus (MMLV) or of the Avian Myeloblastosis Virus (AMV). They differ in size and in their temperature optima. Everything else being the same, one expects a smaller enzyme that is active at a higher temperature to give better RT yields because of more efficient priming. In an absolute quantification study based on an artificial gene an average RT yield of 30% was measured, but it was also found that the yield varied more than 100-fold with the enzyme used and the mRNA target (Ståhlberg et al., 2004b; Peters et al., 2004). Also the priming strategy affects the RT efficiency in a gene specific way. This may sound worrying, suggesting it is difficult to obtain comparable RT QPCR data. But this is not the case. The RT reaction is highly reproducible as long as the same experimental protocol and reaction conditions are used, and results are perfectly comparable (Ståhlberg et al., 2004a). Other sources of variation in quantitative expression analysis are sample preparation and RNA extraction. The variation in losses during RNA isolation between samples can be controlled by spiking the samples with a known concentration of exogenous mRNA. Still, this does not fully mimic the situation of native mRNA molecules that are localized in cell compartments, and we have no idea how the isolation yield varies among different mRNAs. Differences in length, folding, localization in the cell, and complexation to proteins are just some factors that may affect RNA extraction yield.

In mRNA quantification by RT QPCR false positive signals may arise from amplification of the gene or pseudo-gene in genomic DNA. This problem can be avoided by designing the two PCR primers to hybridize to different exons, hence having at least one intron in between, or designing one of the primers to span across an exon/exon boundary (Wang and Seed, 2003). If such designs are not possible the sample should be DNase treated and tested for genomic contamination. This is done by running a no-RT control, which is a normal sample but without reverse transcriptase added.

2.1. The relative gene expression ratio

Comparing samples requires normalization to compensate for differences in the amount of biological material in the tested samples. A number of normalization procedures have been suggested based on physical parameters, such as volume, mass, size and cell number. Due to the heterogeneity of biological samples, these methods are usually unpractical and unreliable. More convenient is to normalize to total RNA amount, to ribosomal RNA, to externally added RNA standard, or to internal reference genes. The latter is currently the most popular strategy. However, finding appropriate reference genes for data normalization is one of the most challenging problems today. Extensive evidence suggests that all genes are regulated under some conditions, and the field will probably have to face that there is no universal reference gene with a constant expression in all tissues (Bustin, 2000; Gibbs et al., 2003). Due to this

uncertainty, any system relying on reference genes should be carefully validated. Panels of potential reference genes are now available for testing (http://www.tataa.com/referencepanels.htm), and softwares have been developed to find the optimal reference genes for defined systems (Pfaffl et al., 2004; Vandesompele et al., 2002). These methods assume that the genes with highest correlated expressions are the most appropriate reference genes. This assumption has the problem that regulated genes may have highly correlated expressions due to co-regulation, and those are not suitable references. The risk of selecting improper reference genes is minimized by choosing genes with different metabolic functions (http://www.tataa.com/referencepanels.htm).

The relative expression of two genes in a same sample is given by Ståhlberg et al. (2005):

$$\frac{N_A}{N_B} = K_{RS} \frac{\eta_B (1 + E_B)^{CT_B - 1}}{\eta_A (1 + E_A)^{CT_A - 1}}$$

(5)

N_A and N_B are the numbers of mRNA molecules of gene A and gene B, respectively, that were present in the test sample. K_{RS} is the relative sensitivity of the detection chemistries of the two assays (Ståhlberg et al., 2003), and η_A and η_B are the cDNA synthesis yields of gene A and gene B, respectively, defined as the fractions of mRNA molecules that are transcribed to cDNA in the RT reaction (Ståhlberg et al., 2004a). The exponent CT-1 accounts for the production of double stranded DNA in the first PCR cycle from the single stranded cDNA template generated by the reverse transcription reaction. η is assumed to be independent of both the total RNA and target mRNA concentrations.

The large number of parameters makes it quite complicated to determine the expression ratio of two genes in a single sample. In most applications the expression ratio of two genes is therefore compared in two or more samples; so called comparative quantification (Pfaffl et al., 2002). Typically, one gene is the reporter whose expression is expected to be affected by the condition studied and the other is a reference gene whose expression should be constant. Assuming the same RT yields in the samples K_{RS} and η cancel and the comparative expression ratio of the two samples is given by

$$\frac{\text{Sample 1}}{\text{Sample 2}} = \frac{\left[\frac{N_A}{N_B}\right]_{\text{Sample 1}}}{\left[\frac{N_A}{N_B}\right]_{\text{Sample 2}}} = \frac{\left[\frac{(1 + E_B)^{CT_B - 1}}{(1 + E_A)^{CT_A - 1}}\right]_{\text{Sample 1}}}{\left[\frac{(1 + E_B)^{CT_B - 1}}{(1 + E_A)^{CT_A - 1}}\right]_{\text{Sample 2}}}$$

(6)

Further assuming that the PCR efficiencies in the two samples are the same the expression simplifies to:

$$\frac{\text{Sample 1}}{\text{Sample 2}} = \frac{(1 + E_B)^{CT_{B1} - CT_{B2}}}{(1 + E_A)^{CT_{A1} - CT_{A2}}}$$

(7)

Finally, one may also assume 100% PCR efficiency. This gives:

$$\frac{\text{Sample 1}}{\text{Sample 2}} = \frac{2^{CT_{B1}-CT_{B2}}}{2^{CT_{A1}-CT_{A2}}} = 2^{(CT_{B1}-CT_{B2})-(CT_{A1}-CT_{A2})} = 2^{\Delta\Delta CT} \tag{8}$$

which is the well-known $\Delta\Delta CT$-method.

2.2. Real-time PCR expression profiling

Characterizing samples through the expression of a single reporter gene normalized with the expression of a reference gene is an excellent approach for many simple studies, but it is not sufficient to classify complex samples. These are traditionally studied using microarray techniques, by which the expression of all the genes is assessed. However, in most cases it is not important to measure the expression of all the genes. In most tissues under reasonably well defined conditions only a fraction of the genome is active, and a limited number of genes have their transcriptional levels significantly altered by external stimuli or moderate environmental changes. A powerful experimental strategy for expression profiling is therefore to first study a small number of representative samples using microarray technology to identify the genes that are most sensitive to the studied condition, and then study these genes in greater detail and in many more samples by the more sensitive and cost efficient real-time PCR technique. Our yet limited experience of real-time PCR expression profiling suggests that the expression of some 20–50 genes catches most of the variation in the expression of the transcriptome under defined study conditions. The selected genes may constitute an expression pathway or a signaling chain, or they can be members of an operon, or respond to a certain environmental change, or reflect a perturbed or disease state of the organism, whose expression can be used to diagnose and classify the disease, and also for making prognosis.

A real-time PCR expression profiling experiment generates a CT value for each gene in each sample that reflects the transcriptional activity of that gene in the particular sample. As we shall see, from such data very valuable and accurate information about the transcriptional response of the studied system can be extracted. Even more powerful experimental design is to study the expression profile of a set of samples also as function of a third parameter such as time after treatment, drug load, etc. Such studies generate so called 3-way data, which are exceedingly informative (Smilde et al., 2004) (http://www.multid.se).

When analyzing the expression of many reporter genes the best approach is to look for characteristic expression profiles. This is a common approach in microarray studies. Having properly selected the genes for the real-time PCR study, expression profiling by real-time PCR has many important advantages to expression profiling by microarrays. Data quality is much better, sensitivity is higher, dynamic range is wider, and all those genes that are not pertinent to the studied conditions and only contribute with noise to the measurement are excluded. Further, the cost for real-time PCR measurements is way lower than for microarray studies, and one can study much larger number of samples and perform more biological repeats with real-time PCR, which is most important for the statistical analysis of data. Usually, the more

significantly expressed genes that are considered the better, but the approach is applicable even for two genes. As shown by Ståhlberg et al., reliable classification of a disease can be obtained by measuring the expression of two marker genes that are reciprocally expressed (Ståhlberg et al., 2003). In their work, summarized in the review by Leijon et al., in this issue, they classified non-Hodgkin lymphoma by measuring the relative expression of the immunoglobulin kappa (IgLκ) and lambda (IgLλ) light chains. The same strategy was recently used to diagnose mantle cell lymphoma by measuring the CCND1:CCND3 expression ratio (Jones et al., 2004).

When classifying data by expression patterns instead of relative expressions, data pre-treatment and normalization become less important. For example, its quite complex to accurately estimate IgLκ:IgLλ expression ratios, which are given by (see Eq. (5)):

$$\frac{N_{\text{IgL}\kappa}}{N_{\text{IgL}\lambda}} = K_{\text{RS}} * \frac{\eta_{\text{IgL}\lambda}(1 + E_{\text{IgL}\lambda})^{\text{CT}_{\text{IgL}\lambda}-1}}{\eta_{\text{IgL}\kappa}(1 + E_{\text{IgL}\kappa})^{\text{CT}_{\text{IgL}\kappa}-1}} \tag{9}$$

Although the unknown parameters can be determined, it is time and resource consuming. If one instead plots the data in a regular scatter plot negative and positive samples are readily distinguished (Fig. 9 in the review by Mikael Leijon et al., in this issue).

2.3. Principal component analysis

A scatter plot is the most intuitive way to visualize the expression of two genes and to classify samples based on their co-expression pattern. Expression of three genes can be visualized in a 3D scatter plot. Studies based on any larger number of genes cannot be directly presented in a scatter plot, because we have no convenient way to plot data in more than three dimensions. To deal with higher order data multivariate chemometric tools are required to reduce the number of dimensions without loss of essential information. A classical, widely available, tool is Principal Components Analysis (PCA), which allows scientists to study many variables simultaneously. PCA not only informs about how the original variables are correlated, but it also shows how the samples are grouped. Principal Components (PCs) are mathematical constructs that can be interpreted as linear combinations of the studied variables with the following important properties:

  (i) The PCs are orthogonal. Once a PC is linked to the behavior of one or several genes, one can be reasonably sure that this information will be unique and these genes will not correlate substantially with other PCs. The numerical coefficients, ranging from −1 to +1, given to each gene in each PC are called loadings and reflect how important the gene is to define this PC.
 (ii) The PCs are sequential. This means that the first and most significant PC can be interpreted as the line in the original multidimensional space of all the genes that best fits the expression data and, hence, explains most of the observed variability and account for most of the information. The second most significant

PC is a vector perpendicular to the first PC that fits the expression data best, and accounts for most of the variability that is not accounted for by the first PC. Additional PCs are defined analogously. This means that one can extract PCs until a certain percentage of all the information, let say 80%, is accounted for, and then discard the remaining PCs.

Once the PCs have been calculated, the samples can be located in this new space. This is done using the scores, which specify the location of each sample on each PC. The original data can now be presented in a simple scatter plot of the scores to reveal groups among the samples or of the loadings to reveal groups among the genes. Many times PC1–PC2 and PC1–PC3 scatter plots are sufficient, but one can also construct PC1–PC2–PC3 scatter plots.

2.4. Data pre-treatment

We assume that all samples are based on, or normalized to, the same amount of material in some way. It can be same amount of total RNA, total mRNA, total cDNA, the same number of cells, body fluid or tissue. We also assume that the data are arranged in a matrix with the genes as columns and the samples as rows.

Real-time PCR raw data are typically expressed in CT values. For classification CTs should be converted to copy numbers using equation:

$$N_0 = (1 + E)^{(CT(sc) - CT)} \tag{10}$$

This requires knowing CT(sc), which is the CT expected for a single template copy sample, and the PCR efficiency. These can be estimated from the slope and intercept of a standard curve (see Eq. (3)), or by calibration using standard additions. Their precise values are not very important for expression profiling by PCA, since the genes and samples are classified by way of their expression patterns, and reasonable estimates are good enough. It is usually sufficient to set all CT values above the lowest CT of primer–dimer signals to this value. Then, when converting CT values to copy numbers, set CT(sc) to the CT of the primer–dimers. PCR efficiencies are usually assay specific and they may also vary from sample to sample. But again classification based on expression profiling is quite insensitive to the efficiency values, and it is usually good enough to assume the same efficiency for all genes in all samples, and set it to a value typical of the particular sample matrix. For blood and many tissue samples this is 0.85–0.90.

Samples are often analyzed in duplicates or even more replicates, and many users average the repeats. For PCA we recommend not averaging repeats, and instead treat them as independent samples. Replicates should lie close to each other in the score plots and their spread gives a very good idea about the reproducibility of the analytical methodology and of each biological replicate.

We must decide if the data shall be analyzed in linear or logarithmic scale. We usually think of the order of enhancement or the order of suppression of expression, which is logarithmic scale. To analyze data in logarithmic scale, we shall calculate the logarithm of the copy numbers. Traditionally in expression profiling this is done

using log with base 2. In $\log_2$ a difference of 2 corresponds to 2-fold increase in expression, 3 corresponds to 4-fold increase, 4 to 8-fold increase, etc., while -2 corresponds to 2-fold reduction. But any other base for the logarithm can also be used.

Next we must decide about normalization. In RT QPCR one often normalizes with the expression of reference genes. However, for PCA this is not necessary. In fact, better classification is usually obtained when the data are not normalized because the normalization adds variance to the data due to the biological variation in the expression of the reference gene(-s). Instead the data can be autoscaled. Typically autoscaling is done for each gene, although the data can also be autoscaled for samples. In autoscaling the mean expression of each gene is first subtracted and then the results are divided by the standard deviation of the expression of each gene. Hence, the autoscaled expression data have zero mean and unit variance for every gene. The consequence of autoscaling is that all genes in the analysis are treated as equally important. Our experience is that autoscaling works very well when the genes are all significantly affected by the studied conditions. Autoscaling is also recommended when the genes are expressed at very different levels. Hence, in summary, we recommend the following data pre-treatment:

(1) Set all CT values that are higher than the lowest CT of primer–dimers to the same value.
(2) Convert CT values to copy numbers assuming an *E* typical of the matrix and CT(sc) to that of the primer–dimers.
(3) Normalize to the same total amount of RNA/cells/blood etc. Optionally normalize with the expression of reference gene(-s).
(4) Convert data to $\log_2$ base.
(5) Autoscale data.

Below we exemplify the procedure by analyzing real-time PCR gene expression profiles of the embryonic development of the African claw frog *Xenopus laevis*.

2.5. Embryonic development in X. laevis

Developmental biology is the effort to describe the relation between mRNA expression, translation and gene function throughout development. RNA expression can be studied on two levels: spatial and temporal distribution. Spatial expression profiles are measured within different organs or different parts of embryos, while temporal expression profiles are measured as function of developmental stage or time. Temporal expression profiling during early development of mammals is limited by the small cellular amounts of protein and RNA (about 20 pg per cell). In contrast, amphibian eggs and embryos, such as those of *X. laevis*, contain several μg of total RNA. This feature further adds to the picture of *X. laevis* as one of the most popular model organisms for developmental studies. Two different groups of mRNA molecules are present during *Xenopus* early development. One group is the maternal mRNA molecules that were expressed during oogenesis and that are present in oocyte already prior to fertilization. Some of the maternal mRNAs (e.g. β-catenin,

VegT, Vg1, Wnt11) are heterogeneously distributed throughout the egg and are responsible for the main body axis formation and germ layer induction (Mowry and Cote, 1999). The second group of mRNA molecules is called zygotic. Zygotic mRNAs are transcribed after a specific developmental phase, which is called mid-blastula transition (MBT) and occurs during the gastrulation process. Among zygotic mRNAs are genes that antagonize bone morphogenetic protein (BMP) and Wnt signaling (e.g. follistatin, cerberus, chordin, noggin), as well as genes that are important for the forthcoming development and organogenesis (e.g. N-CAM and N-tubulin important for neurulation are highly expressed in neural tissue, whereas cardiac actin is expressed in heart tissue).

We have measured the expression of activin, Xbra, cerberus, chordin, derriere, dishevelled, follistatin, goosecoid, GSK3, HNF-3beta, N-CAM, p53, siamois, VegT, Vg1, and Xnot in the *Xenopus* developmental stages 1, 2, 4, 5, 6–7, 8–9, 11, 15, 17, 18–19, 21, 28, 32, 35–36, 41 and 44 assigned according to Nieuwkoop and Faber (1994). This is a total of 16 genes studied in 16 developmental stages. All genes weremeasured in at least duplicates, starting from different samples (biological repeats). In total 39 expression measurements were carried out in 16 developmental stages.

Two sets of three embryos from the different stages were collected from one in vitro fertilization and frozen immediately at $-70\,°C$. RNA from each sample was extracted using Trizol reagent (Invitrogen) according to the instructions of the manufacturer and its concentration was determined by absorption. The RNA quality was analyzed by 1.5% ethidium bromide agarose gel electrophoresis. cDNA was produced starting with 1 µg of total RNA and 10 pmol 25-dT oligo. After incubation at $72\,°C$ for 10 min, 100 U MMLV reverse transcriptase (Promega), 12 U RNasin (Promega) and 5 nmol dNTP were added to a total volume of 10 µl, and incubated at $37\,°C$ for another 70 min. The reactions were subsequently diluted to 200 µl and frozen. The PCR reaction mixture had a final volume of 20 µl and contained 2 µl of cDNA, 10.000-fold diluted SYBR Green solution (Molecular Probes), 0.4 mM forward and reverse primer, 0.3 mM dNTPs, 3 mM $MgCl_2$ and 1 U Taq polymerase (Promega). Real-time PCR data were collected on the BioRad iCycler iQ and the Corbett Research Rotor-Gene 3000 with cycling conditions: $95\,°C$ for 3 min, 40 cycles at $95\,°C$ for 20 s, $60\,°C$ for 20 s, and $72\,°C$ for 20 s. Finally the samples were cooled to $60\,°C$ and a melting curve was recorded between $60\,°C$ and $95\,°C$ with steps of $0.5\,°C$.

Real-time PCR expression measurements are frequently normalized with the expression of reference genes. But this approach is highly unsuitable for development studies, because no gene seems to be expressed at a constant level during development. In a previous study we measured the expression of ODC, EF-1α, L8, GAPDH and H4, which are five popular *Xenopus* reference genes, during development from the egg (stage 1) to the tadpole (stage 44), and found very large variations when normalizing their expressions to the total amount of RNA (Sindelka et al., in press). Autoscaling is therefore much better option.

The RT QPCR data were analyzed using the GenEx software (http://www.multid.se). In the pre-treatment all CT values above 30 were set to 30, which was
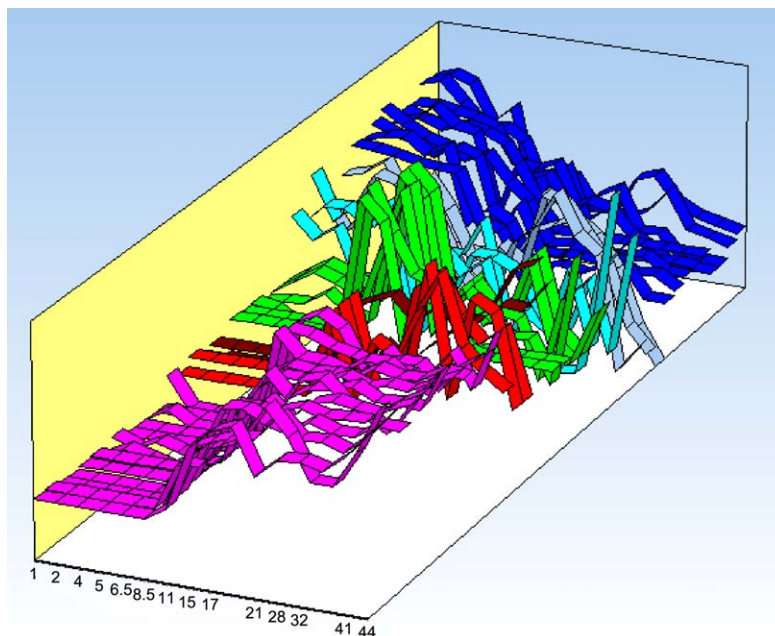
Fig. 10. Expression of *Xenopus laevis* developmental genes during development. Maternal genes are shown in blue (dishevelled, p53, VegT, and Xnot), cyan (Vg1) and sky blue (GSK-3beta), MBT genes are shown in green (Xbra and cerberus), and the late genes are shown in pink (activin, chordin, derriere, follistatin, goosecoid, HNF-3beta, and siamois) and in red (N-CAM). (For interpretation of the references in color in this figure legend, the reader is referred to the web version of this article.)

the lowest CT value observed for primer–dimers. The CT values were then converted to copy numbers assuming a PCR efficiency of 0.90 and CT(sc) = 30. The data were then converted to $\log_2$ scale and autoscaled (Fig. 10).

Principal components were calculated with GenEx, and it was found that the first two PCs account for 76% of the total variation in the data and the first three PCs account for 85% of the variation. Fig. 11 shows the genes in a PC1–PC2 scatter plot. Three groups are seen. In different shades of blue[1] we have the genes dishevelled, GSK-3beta, p53, VegT, Vg1, and Xnot that are expressed in the early stages of development. Genes shown in different shades of red (activin, chordin, derriere, follistatin, HNF-3beta, N-CAM, and siamois) are expressed in late stages. The genes shown in green (Xbra and cerberus) have maximum expression at the MBT stage. By comparing the spread of biological replicates we can distinguish subgroups. In the blue group biological replicates of Vg1 (cyan) and GSK-3beta (sky blue) are distinctly separated from the other early genes. Closer inspection of the expression profiles reveals that both Vg1 and GSK-3beta are expressed also at a later stage of development, while the other early genes are not. Among the late genes the N-CAM repeats

---

[1] For interpretation of color in Figs. 10–13, the reader is referred to the web version of this article.
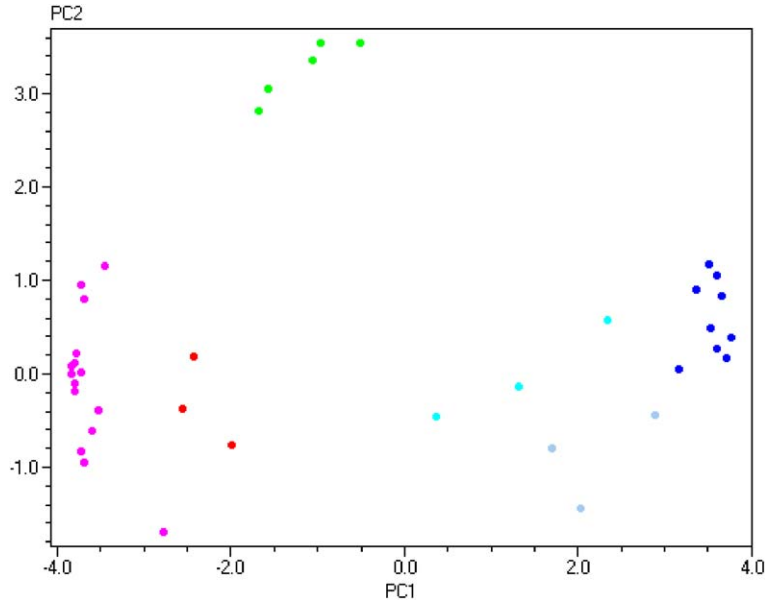
Fig. 11. PC1 vs. PC2 scatter plot of the expression of *Xenopus laevis* developmental genes. Same color coding as in Fig. 10. (For interpretation of the references in color in this figure legend, the reader is referred to the web version of this article.)

(red) are distinct. Closer inspection of the expression data reveals that N-CAM is also highly expressed at MBT, while the other late genes are not. There is one outlier among the pink samples. It is one of the goosecoid biological replicates. Since the other replicate is within the cluster we cannot make any conclusions about biological significance. The groups are even more distinct when viewed in a PC1–PC2–PC3 scatter plot, which accounts for 85% of the variation in the data (Fig. 12).

The stages can also be classified by PCA. Fig. 13 shows the developmental stages in a PC1–PC2 plot classified on the basis of the expressions of the genes. Also here three clusters are evident. First cluster is stages 1–8.5, second cluster is stages 11 and 15, and the third cluster is stages 17–44.

2.6. Single cell gene expression profiling

Cell measurements on tissue or culture in medical research are typically performed on a large number of cells. Gene expression measurements of cell cultures that have been treated differently and comparisons of healthy and abnormal tissues reveal the molecular mechanisms of function and disease. The methods most commonly used require thousands or millions of cells for analysis, and many fundamental breakthroughs in cell biology, physiology and pathology have sprung from these results. However, measuring on a large number of cells limits the findings to population-wide effects and does not address any important information about single cell
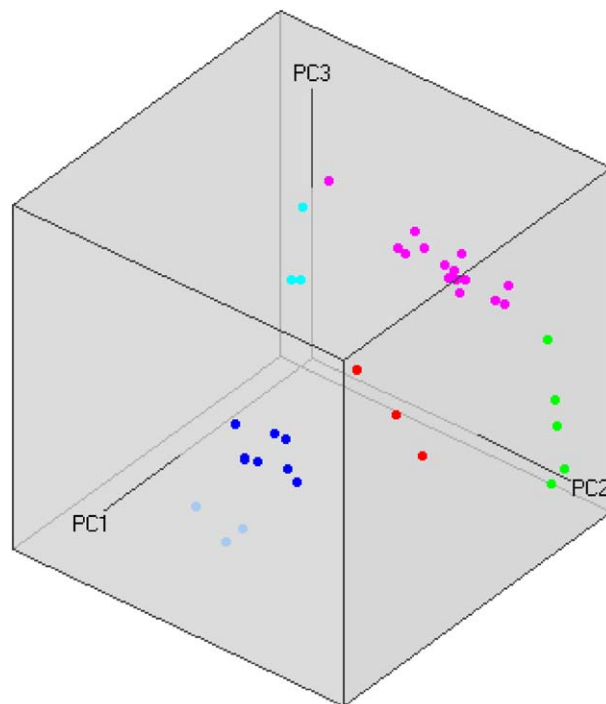
Fig. 12. PC1 vs. PC2 vs. PC3 scatter plot of the expression of *Xenopus laevis* developmental genes. Same color coding as in Fig. 10. (For interpretation of the references in color in this figure legend, the reader is referred to the web version of this article.)

biology. For example, a correlation between the expressions of two genes in a population only tells us that the two genes respond to the same external stimuli at approximately the same way. If we can verify that the correlation is also present on the one cell level, we can conclude that their transcriptional regulations are coupled and perhaps even controlled by the same molecular mechanism.

Another aspect of gene expression measurements is population heterogeneity. Tissues are made of many different cell types that are expected to respond differently to external stimuli and also to be differently affected by disease. In the pancreas, for example, the islets of Langerhans release hormones from at least five cell types, each with distinctly different characteristics (Bishop and Polak, 1997). To fully understand the physiology behind the complex regulatory mechanisms behind biological functions each cell type needs to be studied separately.

Very high sensitivity is required for analysis of transcriptional activity in individual cells. At any one time-point a typical eukaryotic cell contains abut 0.5 pg mRNA. This is equivalent to a few hundred thousand molecules transcribed from about ten thousand genes. To analyze the expression of these genes two methods are available today: In situ hybridization and nucleic acid amplification methods. In situ hybridization studies preserve the morphology of the tissues and expression
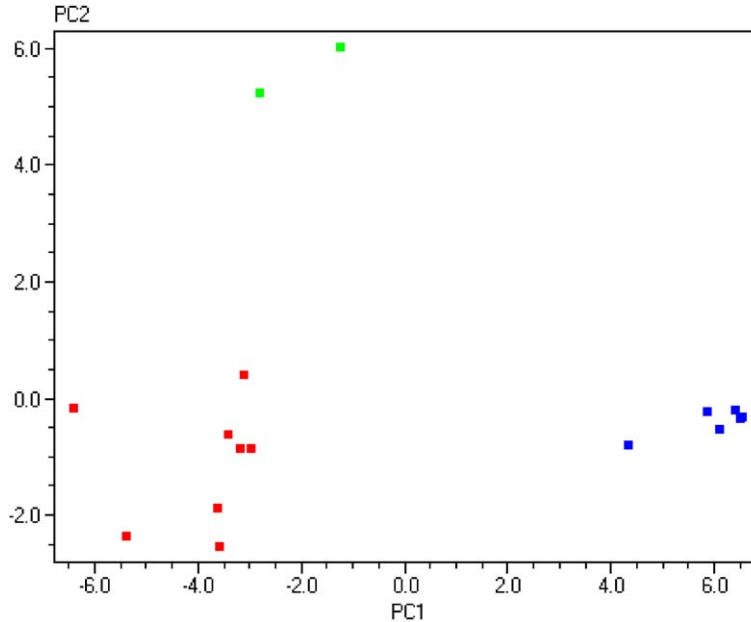
Fig. 13. PC1 vs. PC2 scatter plot of the developmental stages of *Xenopus laevis* classified by the expression of its developmental genes. Stages 1–8.5 are shown in blue, 11–15 in green, and 18.5–44 in red. (For interpretation of the references in color in this figure legend, the reader is referred to the web version of this article.)

is assessed by observing fluorescent probes inside the cell by microscopy (Levsky et al., 2002). Nucleic acid amplification methods are usually variants of either RT-PCR or T7 antisense RNA (aRNA) amplification. The aRNA method is an amplification process where a cDNA library is created from the mRNA, while extending the 5′-end with the T7 promoter sequence. With T7 RNA polymerase large quantities of antisense RNA copies are then produced from the cDNA library, which in turn are reverse transcribed back to cDNA (Wang et al., 2003). In combination with PCR, this method allows for global transcription profiling at the single cell level. However, there is a concern that not all transcripts are amplified with the same efficiency and that the results are biased in unknown way (Nygaard et al., 2003).

RT QPCR is the most versatile method for single cell mRNA analysis and it also offers quantitative information about transcript levels (Bengtsson et al., 2005). High standards on isolation methods are required for proper quantification. For accurate transcriptional profiling all mRNAs from the single cell must make its way to the reaction tube intact and accessible for the reverse transcriptase without introducing inhibitors of the downstream reactions. A number of methods are available. Laser-capture microdissection (LCM) allows handling of μm -sized pieces of tissue without compromising the cellular integrity. The laser beam cuts sections in thin slices of tissue fixed to transfer film, allowing selection based on morphology or staining (see

also the review by Panzini et al., in this issue). Fluorescence activated cell sorting (FACS) is commonly used to sort out a specific cell type from a heterogeneous mixture of cell populations and it can also be used to collect individual cells. Microscopes fitted with micromanipulators are used by electrophysiologists to record currents across membranes in single cells in so called patch-clamp recordings. With minor modifications this setup can be used together with RT QPCR to achieve a powerful combination of functional and transcriptional recordings (Sucher et al., 2000; Liss et al., 2001). For a single cell QPCR in pre-implantation diagnostics, see the review by Traeger-Synodinos in this issue.

As already mentioned the cell-to-cell variation is large even in seemingly homogenous synchronized cell cultures (Levsky and Singer, 2003). Events in the nucleus that determine the fate of the cell are highly probabilistic, or random, in nature. Chemical reactions that involve only a small number of molecules, such as the binding of transcription factors to DNA or the modifications of proteins, are all intrinsically stochastic events. Hence, unlike for the population of cells, the behavior of individual cells cannot be predicted because of a large degree of randomness, or noise that garbles the outcome. This view on gene expression is now established in the field of single cell biology.

We recently studied the transcript levels in a population of insulin producing β-cells and found that a small percentage of the cells express most of the mRNA in the population (Bengtsson et al., 2005). The observed variation was consistent with the lognormal distribution (Fig. 14). This implies that the typical cell in a population
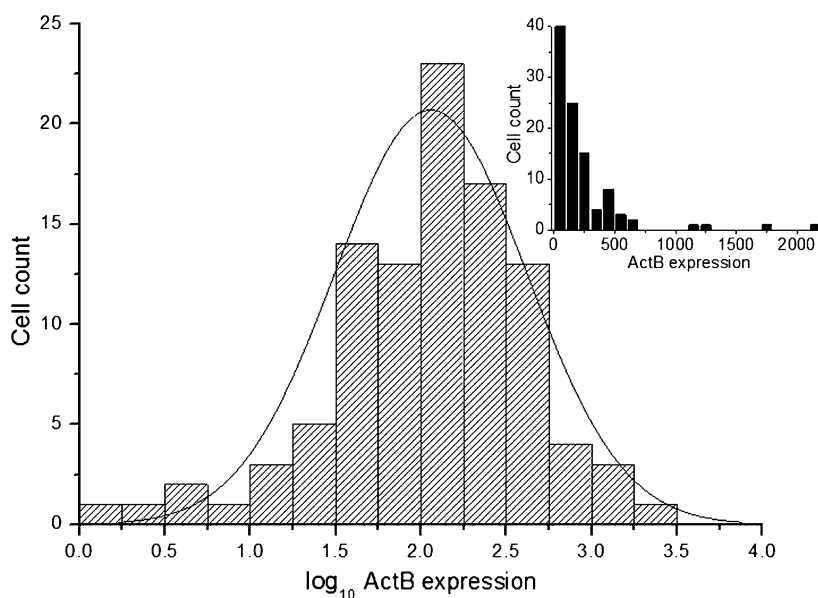

Fig. 14. Lognormal distribution of the expression of ActB in 121 individual β-cells from the pancreas of mouse. Inset shows the distribution in linear scale.

is not well described by the common arithmetic mean of the expression, which is the value measured on a population, but instead by the geometric mean. We further observed that among the five genes studied ActB, Ins1, Ins2, Abcc8, and Kcnj11, only the expressions of Ins1 and Ins2 correlated on the cell level. When glucose was added transcription of Ins1, Ins2 as well as of ActB increased. But ActB was expressed in different cells from those expressing Ins1 and Ins2 (Bengtsson et al., 2005). The origin of the lognormal distributions is unclear, but it has been suggested to arise from multiplicative propagation of fluctuations in correlated equilibria (Furusawa et al., 2005).

Acknowledgement

References

A Nanofluidic Chip for Absolute Quantification of Target Nucleic Acid Sequences. Pharmaceutical Discovery, October 1, 2005.

Akane, A., Matsubara, H., Nakamura, S., Takahashi, S., Kimura, K., 1994. Identification of the heme compound copurified with deoxyribonucleic acid (DNA) from bloodstrains, a major inhibitor of polymerase chain reaction (PCR) amplification. J Forensic Sci. 39, 362–372.

Al-Soud, W.A., Jonsson, L.J., Radström, P., 2000. Identification and characterization of immunoglobulin G in blood as a major inhibitor of diagnostic PCR. J. Clin. Microbiol. 38, 345–350.

BD QZyme™ Assays for Quantitative PCR, 2003. Clontechniques 18 (4), 2–3.

Belgrader, P., Young, S., Yuan, B., Primeau, M., Christel, L.A., Pourahmadi, F., Northrup, M.A., 2001. A battery-powered notebook thermal cycler for rapid multiplex real-time PCR analysis. Anal Chem. 73 (2), 286–289.

Bengtsson, M., Karlsson, J.H., Westman, G., Kubista, M., 2003. A new minor groove binding asymmetric cyanine reporter dye for real-time PCR. Nucleic Acids Res. 31 (8), e45.

Bengtsson, M., Ståhlberg, A., Rorsman, P., Kubista, M., 2005. Gene expression profiling in single cells from the pancreatic islets of Langerhans reveals lognormal distribution of mRNA levels. Genome Res. 15 (10), 1388–1392.

Bishop, A.E., Polak, J.M., 1997. The anatomy, organisation and ultrastructure of the islets of Langerhans. In: Pickup, J., Williams, G. (Eds.), Textbook of Diabetes. Blackwell Science, Oxford, UK, pp. 6.1–6.16.

Bonnet, G., Tyagi, S., Libchaber, A., Kramer, F.R., 1999. Thermodynamic basis of the enhanced specificity of structured DNA probes. Proc. Natl. Acad. Sci. USA 96 (5), 6171–6176.

Braasch, D.A., Corey, D.R., 2001. Locked nucleic acid (LNA): fine-tuning the recognition of DNA and RNA. Chem. Biol. 8 (1), 1–7.

Brenan, C., Morrison, T., 2005. High throughput, nanoliter quantitative PCR. Drug Discovery Today: Technologies 2, 247–253.

Bustin, S.A., 2000. Absolute quantification of mRNA using real-time reverse transcription polymerase chain reaction assays. J. Mol. Endocrinol. 25, 169–193.

Bustin, S.A., 2002. Quantification of mRNA using real-time reverse transcription PCR (RT-PCR): trends and problems. J. Mol. Endocrinol. 29 (1), 23–29.

Caplin, B.E., Rasmussen, R.P., Bernard, P.S., Wittwer, C.T., 1999. LightCycler™ hybridization probes– the most direct way to monitor PCR amplification and mutation detection. Biochemica 1, 5–8.

Costa, J.-M., Ernault, P., Olivi, M., Gaillon, T., Arar, K., 2004. Chimeric LNA/DNA probes as a detection system for real-time PCR. Clin. Biochem. 37, 930–932.

Egholm, M., Buchardt, O., Nielsen, P.E., Berg, R.H., 1992. Peptide nucleic acids (PNA). Oligonucleotide analogs with an achiral peptide backbone. J. Am. Chem. Soc. 114, 1895–1897.

Furusawa, C., Suzuki, T., Kashiwagi, A., Yomo, T., Kaneko, K., 2005. Ubiquity of log-normal distributions in intra-cellular reaction dynamicsBiophysics, Vol. 1. The Biophysical Society of Japan, pp. 25–31.

Gibbs, P.J., Cameron, C., Tan, L.C., Sadek, S.A., Howell, W.M., 2003. House keeping genes and gene expression analysis in transplant recipients: a note of caution. Transpl Immunol. 12 (1), 89–97.

Higuchi, R., Dollinger, G., Walsh, P.S., Griffith, R., 1992. Simultaneous amplification and detection of specific DNA-sequences. Bio-Technology 10 (4), 413–417.

Holland, P.M., Abramson, R.D., Watson, R., Gelfand, D.H., 1991. Detection of specific polymerase chain reaction product by utilizing the $5' \rightarrow 3'$ exonuclease activity of *Thermus aquaticus* DNA polymerase. Proc. Natl. Acad. Sci. USA 88 (16), 7276–7280.

Izraeli, S., Pfleiderer, C., Lion, T., 1991. Detection of gene expression by PCR amplification of RNA derived from frozen heparinized whole blood. Nucleic Acids Res. 19, 6051.

Jansen, K., Nordén, B., Kubista, M., 1993. Sequence dependence of 4′,6-diamidino-2-phenylindole (DAPI)-DNA interactions. J. Am. Chem. Soc. 115, 10527–10530.

Jones, C.D., Darnell, K.H., Warnke, R.A., Zehnder, J.L., 2004. Cyclin D1/Cyclin D3 ratio by real-time PCR improves specificity for the diagnosis of mantle cell lymphoma. J. Mol. Diagn. 6 (2), 84–89.

Kubista, M., 2004. Nucleic acid-based technologies: application amplified. Pharmacogenomics 5 (6), 767–773.

Kubista, M., Zoric, N., 2004. PCR platforms. Encyclopedia of Medical Genomics and Proteomics. Available from: <http://www.dekker.com/servlet/product/DOI/101081EEDGP120020685>.

Kubista, M., Ståhlberg, A., Bar, T., 2001. Light-up probe based real-time Q-PCR. In: Raghavachari, R., Tan, W. (Eds.), Genomics and Proteomics Technologies, Proceedings of SPIE, 4264, pp. 53–58.

Kutyavin, I.V., Afonina, I.A., Mills, A., et al., 2000. 3′-Minor groove binder-DNA probes increase sequence specificity at PCR extension temperatures. Nucleic Acids Res. 28 (2), 655–661.

Levsky, J.M., Singer, R.H., 2003. Gene expression and the myth of the average cell. Trends Cell Biol. 13, 4–6.

Levsky, J.M., Shenoy, S.M., Pezo, R.C., Singer, R.H., 2002. Single-cell gene expression profiling. Science 297, 836–840.

Li, Qingge, Luan, Guoyan, Guo, Qiuping, Liang, Jixuan, 2002. A new class of homogeneous nucleic acid probes based on specific displacement hybridization. Nucleic Acids Res. 30, e5.

Lind, K., Stahlberg, A., Zoric, N., Kubista, M., in press. Combining sequence specific probes and DNA binding dyes in real-time PCR for specific nucleic acid quantification and melting curve analysis. Biotechniques.

Liss, B., Franz, O., Sewing, S., Bruns, R., Neuhoff, H., Roeper, J., 2001. Tuning pacemaker frequency of individual dopaminergic neurons by Kv4.3L and KChip3.1 transcription. EMBO J. 20, 5715–5724.

Mackya, I.M., 2004. Real-time PCR in the microbiology laboratory. Clin. Microbiol. Infect. 10, 190–212.

Mattarucchi, E., Marsoni, M., Binelli, G., Passi, A., Lo Curto, F., Pasquali, F., Porta, G., 2005. Different real time PCR approaches for the fine quantification of SNP's alleles in DNA pools: assays development, characterization and pre-validation. J. Biochem. Mol. Biol. 38 (5), 555–562, Sep 30.

Mhlanga, M.M., Malmberg, L., 2001. Using molecular beacons to detect single-nucleotide polymorphisms with real-time PCR. Methods 25 (4), 463–471.

Mowry, K.L., Cote, C.A., 1999. RNA sorting in *Xenopus* oocytes and embryos. FASEB J. 13 (3), 435–445.

Nazarenko, I., Lowe, B., Darfler, M., Ikonomi, P., Schuster, D., Rashtchian, A., 2002. Multiplex quantitative PCR using self-quenched primers labelled with a single fluorophore. Nucleic Acids Res. 30 (9), e37.

Nieuwkoop, P.D., Faber, J., 1994. Normal Table of *Xenopus laevis*. Garland Publishing, Inc., New York, London.

Nygaard, V., Loland, A., Holden, M., Langaas, M., Rue, H., Liu, F., Myklebost, O., Fodstad, O., Hovig, E., Smith-Sorensen, B., 2003. Effects of mRNA amplification on gene expression ratios in cDNA experiments estimated by analysis of variance. BMC Genomics 4, 11.

Nygren, J., Svanvik, N., Kubista, M., 1998. The interaction between the fluorescent dye thiazole orange and DNA. Biopolymers 46, 39–51.

Peters, I.R., Helps, C.R., Day, M.J., 2004. Real-time RT-PCR: considerations for efficient and sensitive assay design. J. Immunol. Methods 286 (1-2), 203–217.

Pfaffl, M.W., Horgan, G.W., Dempfle, L., 2002. Relative expression software tool (REST) for groupwise comparison and statistical analysis of relative expression results in real-time PCR. Nucleic Acids Res. 30 (9), E36.

Pfaffl, Michael W., Tichopád, Aleš, Prgomet, Christian, Neuvians, Tanja P., 2004. Determination of stable housekeeping genes, differentially regulated target genes and sample integrity: BestKeeper—Excel-based tool using pair-wise correlations. Biotechnol. Lett. 26, 509–515.

Primer3. Available from: <http://frodo.wi.mit.edu/..cgi-bin/primer3/primer3_www.cgi>. Netprimer. Available from: <http://www.premierbiosoft.com/netprimer>.

Ririe, K.M., Rasmussen, R.P., Wittwer, C.T., 1997. Product differentiation by analysis of DNA melting curves during the polymerase chain reaction. Anal. Biochem. 245 (2), 154–160.

Rutledge, R.G., 2004. Sigmoidal curve-fitting redefines quantitative real-time PCR with the prospective of developing automated high-throughput applications. Nucleic Acids Res. 32, e178.

Rutledge, R.G., 2005. Sigmoidal curve-fitting redefines quantitative real-time PCR with the prospective of developing automated high-throughput applications. Nucleic development of a kinetic-based sigmoid model for the polymerase chain reaction and its application to quantitative PCR. In: 2nd International qPCR Symposium, Freising.

Rutledge, R.G., Cote, C., 2003. Mathematics of quantitative PCR and the applications of standard curves. Nucleic Acids Res. 31, e93.

Simonson, T., Pecinka, P., Kubista, M., 1998. DNA tetraplex formation in the control region of c-myc. Nucleic Acids Res. 26, 1167–1172.

Simonsson, T., 2001. G-Quadruplex DNA structures—variations on a theme. Biol. Chem. 382, 621.

Sindelka, R., Ferjentsik, Z., Jonák, J., in press. Developmental expression profiles of Xenopus laevis reference genes. Dev. Dyn.

Sjöback, R., Nygren, J., Kubista, M., 1995. Absorption and fluorescence properties of fluorescein. Spetrochim. Acta Part A 51, L7–L21.

Smilde, A., Bro, R., Geladi, P., 2004. MultiWay Analysis. John Wiley & Sons Ltd., ISBN 0-471-98691-7.

Ståhlberg, A., Åman, P., Ridell, B., Mostad, P., Kubista, M., 2003. Quantitative real-time pcr method for detection of B-lymphocyte monoclonality by comparison of k and l immunoglobulin light chain expression. Clin. Chem. 49, 51–59.

Ståhlberg, A., Håkansson, J., Xian, X., Semb, H., Kubista, M., 2004a. Properties of the reverse transcription reaction in mRNA quantification. Clin. Chem. 50 (3), 509–515.

Ståhlberg, A., Kubista, M., Pfaffl, M., 2004b. Comparison of reverse transcriptases in gene expression analysis. Clin. Chem. 50 (9), 1678–1681.

Ståhlberg, A., Zoric, N., Åman, P., Kubista, M., 2005. Quantitative real-time PCR for cancer detection: the lymphoma case. Expert Rev. Mol. Diagn. 5, 221–230.

Sucher, N.J., Deitcher, D.L., Baro, D.J., Warrick, R.M., Guenther, E., 2000. Genes and channels: patch/voltage-clamp analysis and single-cell RT-PCR. Cell Tissue Res. 302, 295–307.

Svanvik, N., Westman, G., Dongyuan, W., Kubista, M., 2000. Light-up probes thiazole orange conjugated PNA for detection of nucleic acid in homogeneous solution. Anal. Biochem. 281, 26–35 http://www.lightup.se.

Tyagi, S., Kramer, F.R., 1996. Molecular Beacons: probes that fluorescence upon hybridization. Nat. Biotechnol. 14 (3), 303–308.

Tyagi, S., Bratu, D.P., Kramer, F.R., 1998. Multicolor molecular beacons for allele discrimination. Nat. Biotechnol. 16 (1), 49–53.

Uehara, H., Nardone, G., Nazarenko, I., Hohman, R.J., 1999. Detection of telomerase activity utilizing energy transfer primers: comparison with gel- and ELISA-based detection. Biotechniques 26 (3), 552–558.

Van, T.-L., Paquet, N., Calvo, E., Cumps, J., 2005. Improved real-time RT PCR method for high throughput measurements using second derivative calculations and double correction. Biotechniques 38, 287–293.

Vandesompele, J., De Preter, K., Pattyn, F., Poppe, B., Van Roy, N., De Paepe, A., Speleman, F., 2002. Accurate normalization of real-time quantitative RT-PCR data by geometric averaging of multiple internal control genes. Genome Biol. 3 (7), 0034.I–0034.II.

Wang, X., Seed, B., 2003. A PCR primer bank for quantitative gene expression analysis. Nucleic Acids Res. 31 (24), e154.

Wang, J., Hu, L., Hamilton, S.R., Coombes, K.R., Zhang, W., 2003. RNA amplification strategies for cDNA microarray experiments. Biotechniques 34, 394–400.

Whitcombe, D., Theaker, J., Guy, Sp., Brown, T., Little, S., 1999. Detection of PCR products using self-probing amplicons and fluorescence. Nat. Biotechnol. 17 (8), 804–807.

Wilson, R., Johansson, M.K., 2003. Photoluminescence and electrochemiluminescence of a Ru(II) (bpy)3-quencher dual-labeled oligonucleotide probe. Chem. Commun. 21, 2710–2711.

Wittwer, C.T., Herrmann, M.G., Gundry, C.N., Elenitoba-Johnson, K.S., 2001. Real-time multiplex PCR assays. Methods 25 (4), 430–442.

Zipper, H., Brunner, H., Bernhagen, J., Vitzthum, F., 2004. Investigations on DNA intercalation and surface binding by SYBR Green I, its structure determination and methodological implications. Nucleic Acids Res. 32 (12), e103.